Jefferson Lab
E94010 Technical Note 31
May 02 2000

Shower Detector Calibration and Cut Optimization for E94010

K. Slifer
Temple University, Philadelphia, PA 19122

E-mail
slifer@jlab.org

Calibration of the Hall A HRS calorimeters for experiment E94010 is discussed. An optimization of the particle i.d. cut is performed, taking into account the cut efficiency and resulting pion contamination. Also, the detection efficiency of the calorimeters is measured.

Contents

1 Introduction

An electromagnetic cascade of energetically degraded secondaries (γ,e^+,e^-) results when an energetic particle enters a dense material. As the cascade propagates, most of the original particle's energy is converted to heat and light. A calorimeter or "shower detector", relies upon collection of this light to determine a particle's energy. The calorimeter is typically segmented into many individual cells or blocks with each block being monitored by a photomultiplier tube. Subsequently, a transformation must be made from raw ADC of the phototubes to the total energy deposition of the incident particle. This transformation is accomplished by determining calibration coefficients for each of the detector blocks. Since the cascade is in general spread laterally over several adjacent blocks, the output must be integrated over the entire detector volume to obtain the total detectable signal. When the calorimeter has been calibrated properly, the total deposited energy E, will agree with the particle's incident energy (or momentum p in the relativistic case). A plot of E/p will look like Fig. 1.

The basic phenomenon of the shower development is statistical in nature so that the E/p peak obtained from each individual block will possess an intrinsic width. The width σ of the total E/p peak thus gives a measure of how properly the individual blocks have been aligned by the calibration.

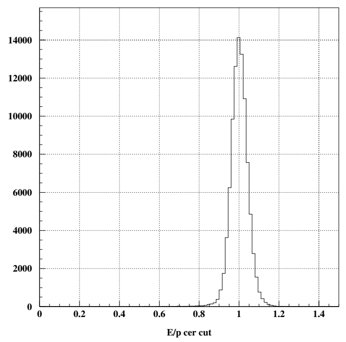

Figure 1: E/p for properly calibrated shower

1.1 Selection of good events

In the analysis of both Electron and Hadron arm shower detectors a geometrical cut on the variables, ϕ, y-Target, θ,and δP has been applied to eliminate events originating from the target glass endcaps, and other bad events (Fig. 2). The same cut is used in the final physics analysis.

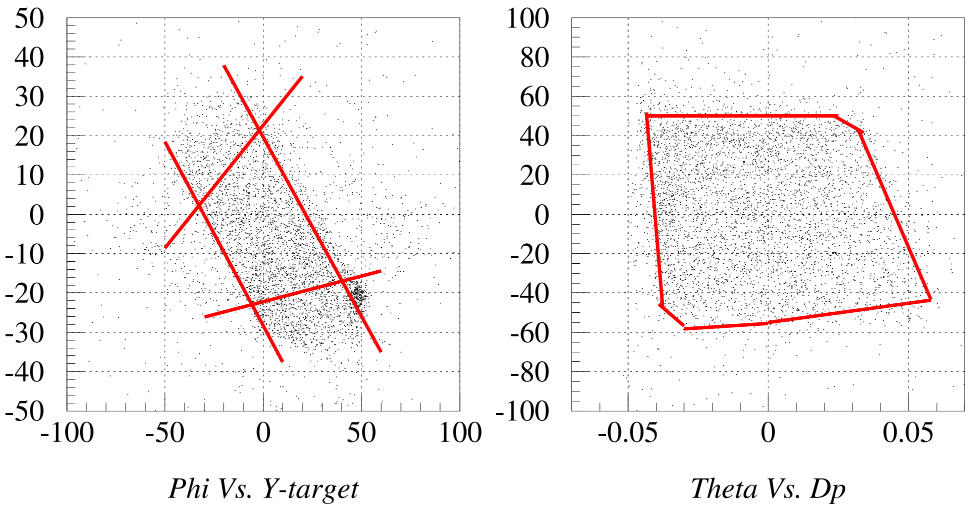

Figure 2: Geometrical Cut used in the Analysis

2 Electron Arm

2.1 Electron Arm Shower Detector Details

The electron arm HRS calorimeter consists of two segmented layers. The first "preshower" layer is made of 48(24×2) blocks of TF-1 lead glass. Each of the preshower blocks are 10cm.×10cm.×35cm. The second shower layer is made of 96(48×2) blocks of SF-5 lead glass. Each of the shower blocks are 15cm.×15cm.×35cm. [1]

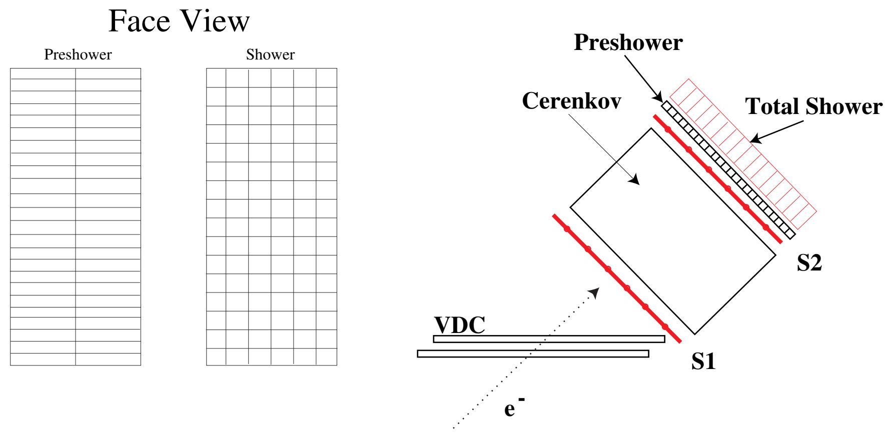

Figure 3: Electron arm HRS Detector package

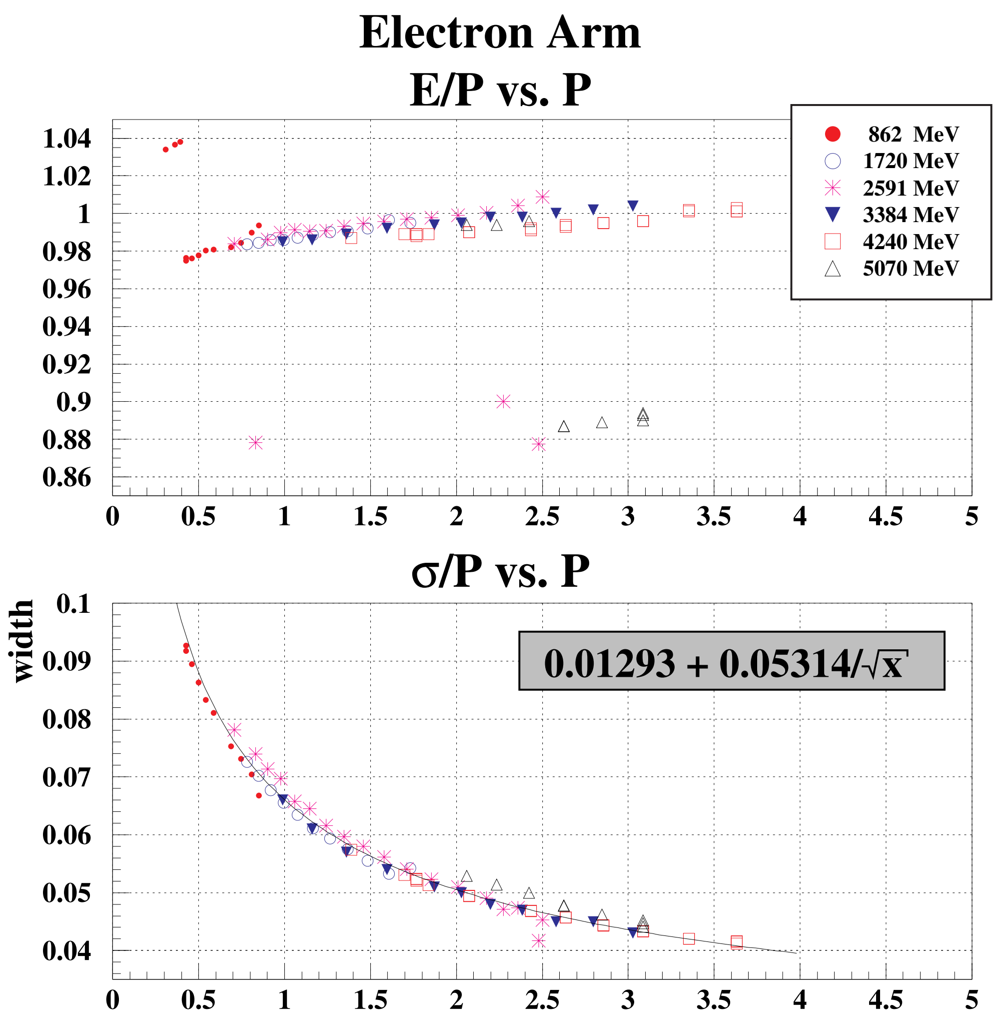

Figure 4: Calibrated Shower Output for Electron Arm

2.2 Calibration

The calibration procedure is discussed in detail in Ref. [1]. The standard method entails generation of a new calibration for every kinematic investigated. This can be a lengthy process and becomes unreliable when there are hardware problems with any of the blocks or phototubes, as there were during certain runs of E94010. As an alternative, a single set of calibration constants was created, optimized for one well behaved mid-momentum range run (20411, E_0= 2.591 GeV,P_0= 1.579 GeV/c), and then applied to all the data. This poses no disadvantage when we use the shower for electron/pion discrimination since the shower response varies only slightly with momentum. Fig. 4 shows the peak position, E/p, and normalized width, σ/E, for each spectrometer setting once the calibration has been applied. The six data sets represent the various incident energies of E94010. A variation of less than 3% in peak position is seen for most of the runs. The low outliers represent data taken late

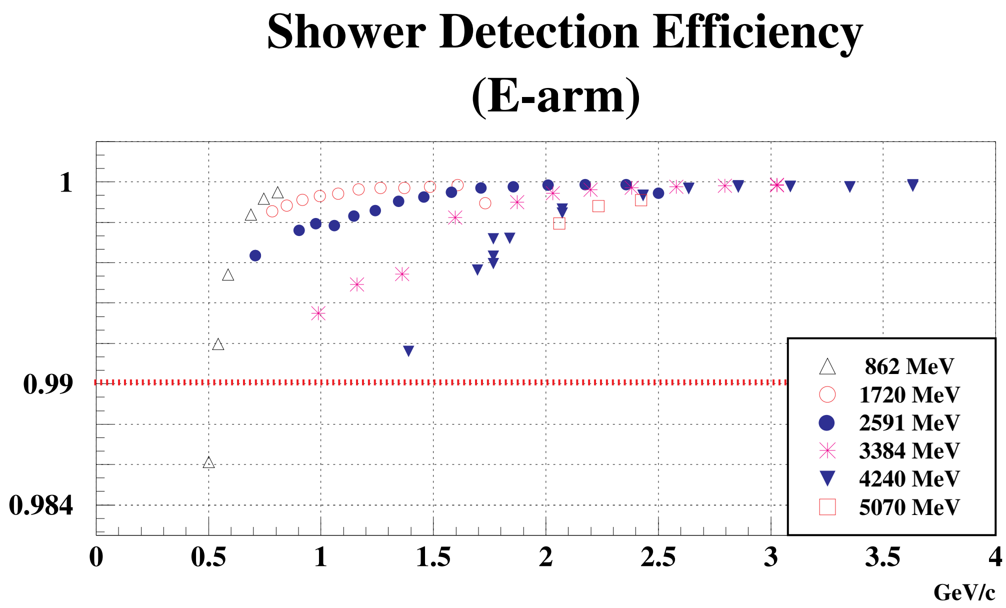

Figure 5: Detection Efficiency of Electron Arm Total Shower

in the experiment (Dec. 11-21, 1998) when the scintillator detector threshold was lowered. Since the scintillator provides the trigger, lowering the threshold allowed more low energy particles into the data. The data with larger than normal E/p represent data taken near the limits of the spectrometer field settings. Here, the dipole NMR probe becomes unreliable so the gaussmeter was used instead. The difference presumably reflects an offset in the value calculated for p using the gaussmeter. These data runs also suffer from the inefficiency caused by the Espace shower cluster formation algorithm. (See Fig. 6 and the discussion in 2.3)
The shower development is a statistical processes, hence the energy resolution of the calorimeter, expressed in terms of the normalized width σ/E, improves with increasing energy. The measured resolution

$$\sigma/E \sim 0.05/\sqrt{E} \tag{1}$$

agrees well with expectation [2].

2.3 Detection Efficiency

Good electrons are selected from T1 events with the previously mentioned geometrical cut along with the requirement of the Čerenkov detector being triggered. The preshower and shower sections are then considered as a single composite detector. An efficiency is calculated for the total calorimeter by counting the number of events that fire the Čerenkov and comparing this to the number of events that trigger *both* the preshower and shower. The detection efficiency was greater than 99% for all incident energies of E94010 except for the

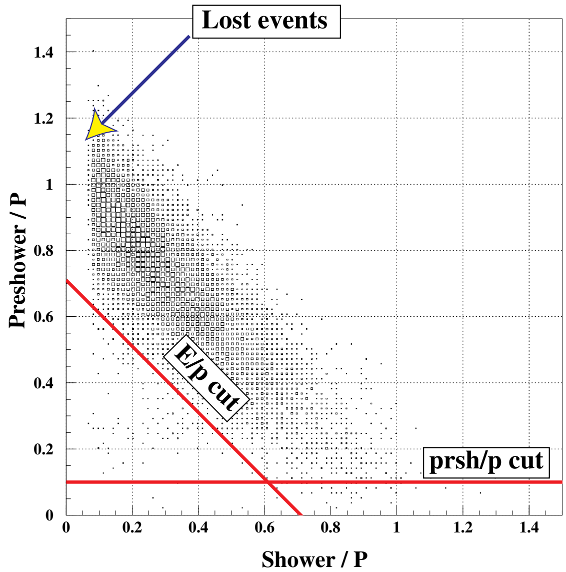

Figure 6: Loss of events at low Momentum, 862 MeV

low momentum settings of 862 MeV (Figs. 5, 6). In the upper left portion of Fig. 6 we can see that a large number of events with a low shower energy deposition are excluded by the cluster formation algorithm and the efficiency is degraded. In this case, the Espace shower cluster variables spec_e.show.cl_e,and spec_e.preshow.cl_e should be replaced by the pre-clusterized values of the ADC output. It can be seen in Fig. 5 that there is a slight dependence of the total shower detection efficiency on ν=E-E'.

2.4 Cut Efficiency

Both an E/p and preshower/p cut are utilized, and both can introduce inefficiencies by excluding good electrons. These two cuts can also be seen in Fig. 6, although there are no visible pions in this plot. To measure the total cut efficiency, all good events excluded by the cut must be estimated, ensuring that events excluded by both cuts are not counted twice. The choice of the cuts was optimized so that the pion suppression is large, while the total cut inefficiency always remains less than 1%.

2.5 Pion Contamination

Detection of Čerenkov light as a charged particle passes through a transparent medium provides an excellent method of particle identification, since the threshold for Čerenkov light production is highly sensitive to the mass of the particle. Thus, pions can be excluded from data by use of the HRS gas Čerenkov detectors. The Čerenkov detector gas is chosen such that any electrons above 17 MeV/c will trigger the detector, while a pion must have momentum above 4.8 GeV/c to generate Čerenkov light in the gas medium [4]. Calibration of the Čerenkov detectors has been performed and the electron detection efficiency has been determined for all the kinematics of E94010 [3].

Because pions have a characteristic energy deposition in the calorimeter, cuts on the preshower and shower can also be used to eliminate pions from the data. Once these three cuts have been applied, an estimate of residual pion contamination is neccessary. This value will include any knock-on electrons ejected by incident pions within the detector package. While the π/e ratio can be as great as 5 for some kiematics , a modest E/p cut typically reduces this to less than a few percent without help from the Čerenkov or preshower cuts. These latter cuts typically suppress the pions by another two orders of magnitude. The resulting pion contamination is negligible for all but a few E94010 kinematics (See Tables 1-12).

2.5.1 Pion Suppression by a Cut on the Preshower Detector

The pion suppression obtained by a preshower cut is measured by using an anti-Čerenkov cut to tag pions in the shower and then measuring the ratio of pions before and after the preshower cut. A factor of 4-5 is typically obtained with a modest preshower cut. See Fig. 7A.

2.5.2 Pion Suppression by a Cut on the Čerenkov Detector

It is not as simple to measure the Čerenkov's ability to suppress pions, as we must now rely on the shower to identify pions before the cut. Complications also arise when attempting to fit pions in an E/p plot. The pronounced pion peak is mainly due to the energy deposition in the preshower, as it is much too thin to absorb all of the pion's energy. Roughly the same amount is sampled from any incident pions in the preshower, while a pion's energy deposition is spread over a much wider range in the thicker second stage of the shower. In addition, the Čerenkov suppression is so strong that any attempt to fit residual pion peaks is particularly difficult unless extremely large statistics are used.

Nevertheless, a simple method can be used to obtain a conservative estimate (hereafter called γ_{cer}) of the true Čerenkov suppression factor γ_{real}. We count all events N_i excluded by an E/p cut. The majority of these excluded events, shown in Fig. 7B, are pions.

$$N_i = \pi_i + e_i \tag{2}$$

where

π_i is the number of initial pions excluded by the E/p cut.

$e_i = \epsilon \cdot \pi_i$: Number of initial electrons excluded by the E/p cut.

Now a Čerenkov cut is applied to this excluded data sample and we have

$$N_f = \pi_f + e_f \tag{3}$$

π_f: Number of remaining pions excluded by the E/p cut.

$e_f = \delta \cdot \pi_f$: Number of final electrons excluded by the E/p cut.

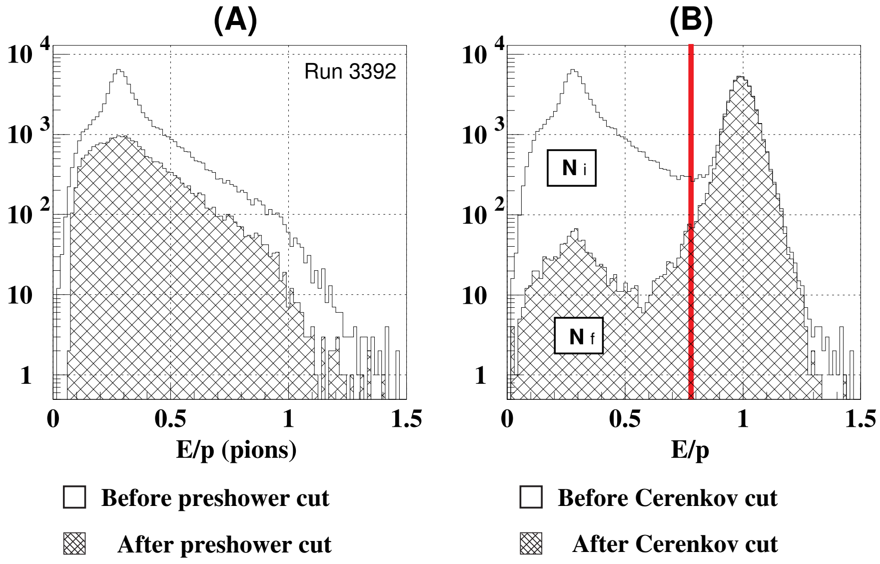

Figure 7: Measuring π suppression.

Electrons are not affected by the Čerenkov cut so:

$$e_i = e_f \tag{4}$$

$$\epsilon \cdot \pi_i = \delta \cdot \pi_f \tag{5}$$

$$\frac{\epsilon}{\delta} = \frac{\pi_f}{\pi_i} \leq 1 \tag{6}$$

Now, assuming the worst case scenario, that is, all the events excluded by the E/p cut are pions, we define γ_{cer}:

$$\gamma_{cer} = \frac{N_i}{N_f} = \frac{\pi_i}{\pi_f} \cdot \frac{(1+\epsilon)}{(1+\delta)} \tag{7}$$

and since

$$\gamma_{real} = \frac{\pi_i}{\pi_f} \tag{8}$$

we can conclude that

$$\gamma_{cer} \leq \gamma_{real} \tag{9}$$

The value γ_{cer} is always less than the true Čerenkov pion suppression so the values quoted in Tables 1-12 for final pion contamination are conservative. In the limit of no pions present in the data sample, $\gamma_{cer} \to 1$, which explains the apparent poor suppression factors for some kinematics shown in the attached tables. On the other hand, for the kinematics were pion production is large, δ and ϵ are small corrections, and $\gamma_{cer} \to \gamma_{real}$.

2.5.3 Residual pion contamination

The value of final pion contamination is given by the ratio π/e inside the E/p cut, divided by the preshower and Čerenkov suppression factors.

3 Hadron Arm

3.1 Hadron Arm Shower Detector Details

The Hadron arm shower detector consists of a single layer of 32(16×2) lead glass blocks arranged as shown in Fig. 8

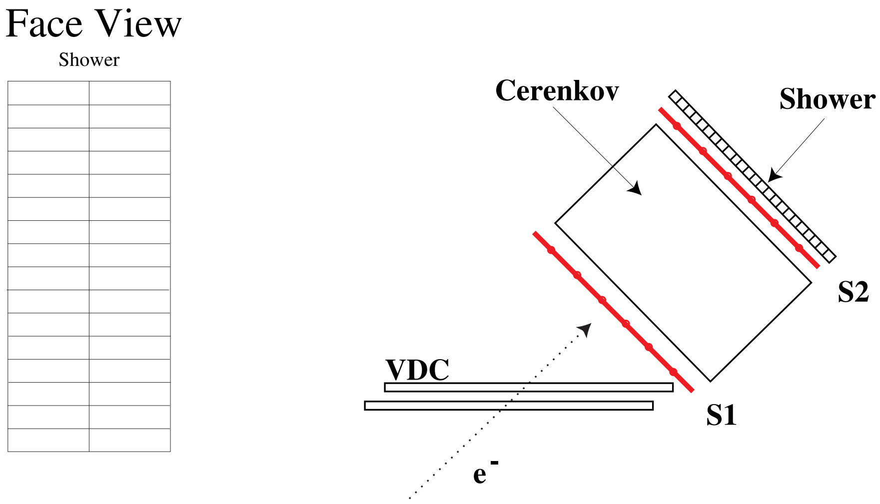

Figure 8: Hadron Arm Detector Package

3.2 Calibration

The Hadron arm lacks a total shower so the method utilized for the Electron arm calibration is not possible. As an alternative, good electron events where only one block has been fired are selected. The software gain of each block is then manually adjusted to set the shower output normalized by particle momentum to unity. Again, a single calibration was

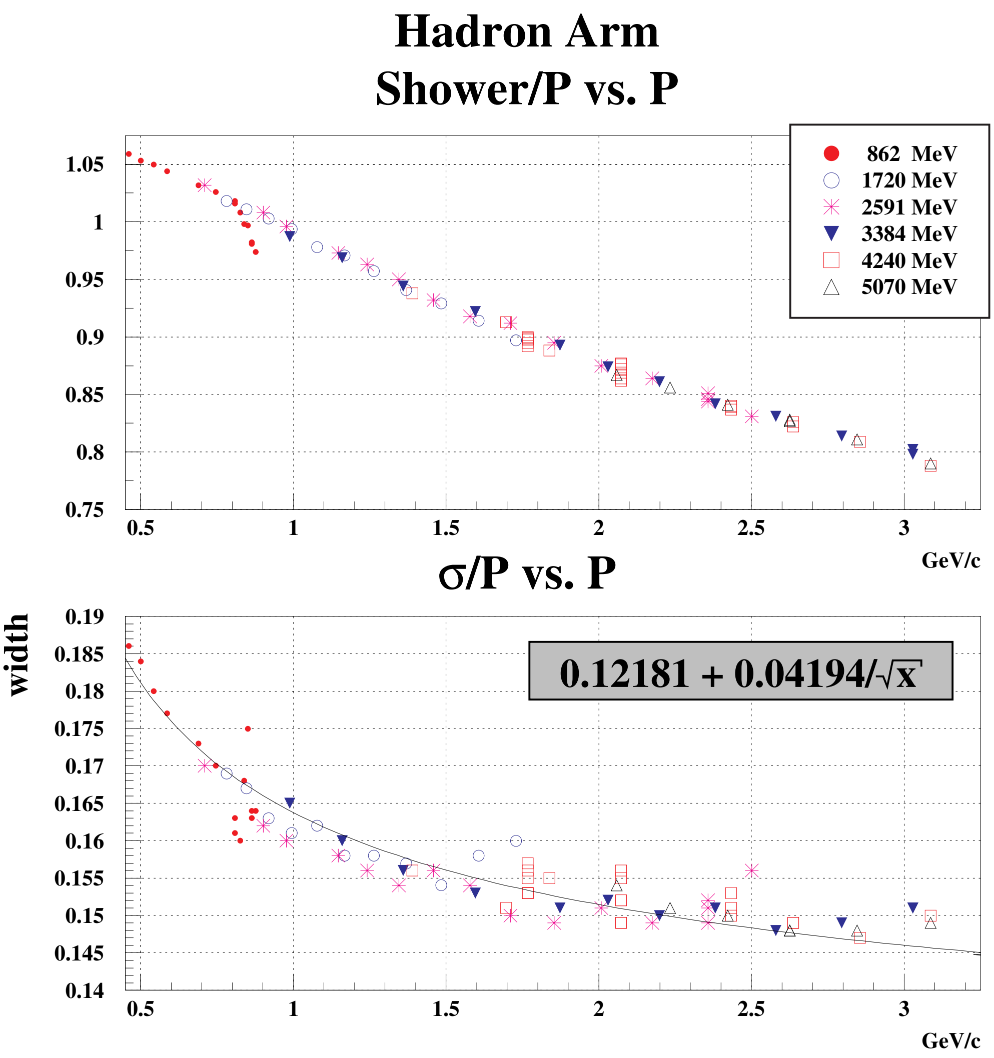

Figure 9: Calibrated Shower Output for Hadron Arm

performed and the result applied to all kinematics. The resulting shower output is then tracked throughout the experiment. (See Fig. 9.) Here the ratio of shower/p decreases with increasing momentum, as only a small portion of the scattered particle's energy is sampled by the detector. Again we see that the width decreases with increasing energy, although the resolution σ/E is much poorer than in the electron arm shower detector.

3.3 Detection Efficiency

The detection efficiency of the Hadron arm shower suffers due to the loss of electrons that pass through the spacing between the vertical columns of blocks. Nevertheless, the detection efficiency is found to be greater than 99% for all of E94010 (See Fig. 10.)

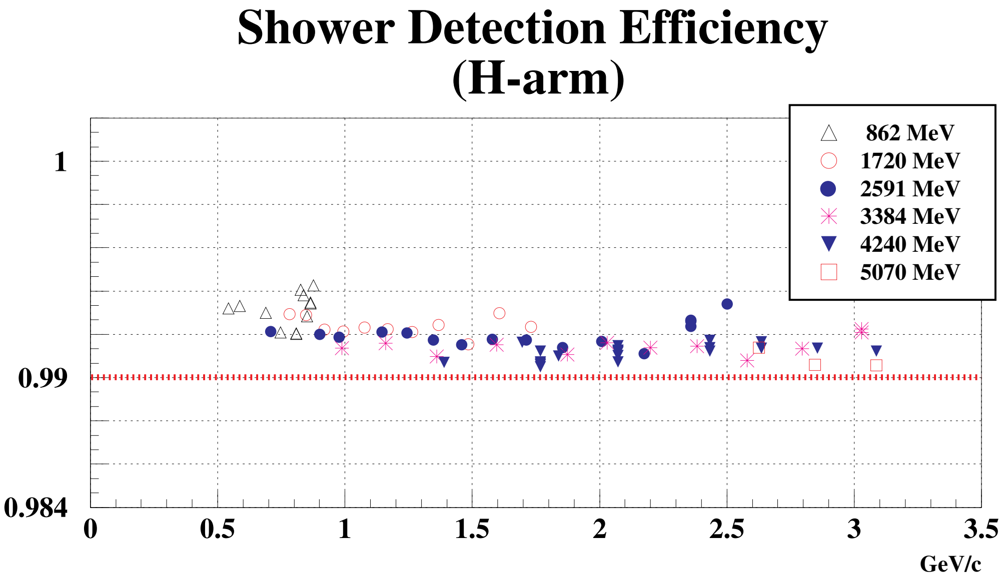

Figure 10: Detection Efficiency of Hadron Shower Detector

3.4 Cut Efficiency

The Hadron arm shower cut is chosen so that the cut inefficiency is $\leq$0.5 % to accomadate the large detection inefficiency. Good electrons that have passed through the spacing of the Hadron blocks will be incorrectly removed by any cut on the Hadron shower since they produce no output in the detector. However, this category of events represent less than 1% of the total data as stated in section (3.3) so the loss is extremely small. A maximum of 1.5% of good events will therefore be excluded by the cut.

4 Conclusion

The Hall A HRS calorimeters have been calibrated and shown to be stable throughout experiment E94010. Detection inefficiencies were found to be small but not always negligible. Detection efficiency is poor for the low momenta runs with 862 MeV incident energy in the Electron arm. The Hadron arm loses more good electrons in the shower detector in general, due to the air gap between the vertical columns of blocks. The detection efficiency was nevertheless greater than 99% for both detectors for most of E94010. Cut efficiencies have been optimized and the resulting pion contamination is found to be negligible for most kinematics.

5 Data Tables

Here we list the results of the shower analysis. The table entries are explained as follows:

$(\pi/e)_{raw}$: the initial pion to electron ratio with only the geometricial cut, (Fig. 2), applied.

$(\pi/e)_{in}$: π/e after introduction of E/p cut.

Tot Cut Eff. : Total Efficiency of joint E/p and Psh/p cut.

$(\pi/e)_f$: Final π/e ratio, after all cuts.

γ_{prs} : Preshower pion suppression factor.

γ_{cer} : Cerenkov pion suppression factor.

Det Eff : Detection Efficiency.

5.1 Electron Arm Results

Table 1: Electron Arm, 860 MeV

p_0 (GeV)	$(\pi/e)_{raw}$	$(\pi/e)_{in}$	psh/p cut	E/p cut	Tot Cut Eff	$(\pi/e)_f$	γ_{prs}	γ_{cer}	Det Eff
0.851									
0.808	0.00144	0.00132	0.130	0.76	0.9903	0.105E-02	1.22	1.03	0.99949
0.746	0.00404	0.00300	0.130	0.77	0.9903	0.138E-02	1.66	1.31	0.99916
0.689	0.00880	0.00606	0.130	0.77	0.9903	0.257E-02	1.43	1.65	0.99839
0.587	0.01153	0.00800	0.130	0.75	0.9903	0.437E-02	1.08	1.70	0.99542
0.542	0.01232	0.00866	0.130	0.74	0.9903	0.454E-02	1.05	1.82	0.99198
0.500	0.01314	0.00924	0.100	0.73	0.9902	0.483E-02	1.02	1.88	0.98613
0.461	0.01398	0.00969	0.100	0.72	0.9902	0.512E-02	1.02	1.86	0.97731
0.426	0.01311	0.00943	0.100	0.71	0.9902	0.515E-02	1.02	1.79	0.96294
0.393	0.01334	0.00964	0.100	0.75	0.9902	0.532E-02	1.01	1.79	0.95935
0.363	0.01170	0.00891	0.100	0.74	0.9902	0.515E-02	1.02	1.70	0.93889
0.309	0.00857	0.00681	0.100	0.71	0.9902	0.441E-02	1.03	1.50	0.87855

Table 2: Electron Arm, 1.720 GeV									
p_0 (GeV)	$(\pi/e)_{raw}$	$(\pi/e)_{in}$	psh/p cut	E/p cut	Tot Cut Eff	$(\pi/e)_f$	γ_{prs}	γ_{cer}	Det Eff
1.730	0.00089	0.00064	0.110	0.79	0.9906	0.484E-03	1.27	1.04	0.99895
1.607	0.00139	0.00068	0.115	0.79	0.9903	0.309E-03	1.90	1.16	0.99983
1.484	0.00860	0.00089	0.120	0.79	0.9900	0.772E-04	4.49	2.56	0.99975
1.369	0.01738	0.00107	0.120	0.80	0.9908	0.528E-04	5.45	3.72	0.99971
1.264	0.03482	0.00185	0.125	0.79	0.9907	0.416E-04	6.67	6.65	0.99971
1.167	0.07448	0.00305	0.130	0.79	0.9906	0.354E-04	6.92	12.43	0.99964
1.077	0.12037	0.00503	0.130	0.79	0.9907	0.420E-04	6.92	17.27	0.99942
0.994	0.16056	0.00794	0.140	0.78	0.9905	0.392E-04	8.12	24.93	0.99930
0.918	0.19140	0.01233	0.140	0.78	0.9903	0.537E-04	8.34	27.53	0.99912
0.847	0.23170	0.02902	0.145	0.76	0.9907	0.108E-03	8.07	33.16	0.99883
0.782	0.26893	0.05734	0.150	0.76	0.9902	0.228E-03	7.41	33.89	0.99855

Table 3: Electron Arm, 2.591 GeV									
p_0 (GeV)	$(\pi/e)_{raw}$	$(\pi/e)_{in}$	psh/p cut	E/p cut	Tot Cut Eff	$(\pi/e)_f$	γ_{prs}	γ_{cer}	Det Eff
2.501	0.00092	0.00041	0.085	0.85	0.9909	0.207E-03	1.87	1.06	0.99944
2.357	0.00136	0.00053	0.085	0.84	0.9907	0.216E-03	2.18	1.13	0.99987
2.175	0.00830	0.00072	0.090	0.83	0.9910	0.837E-04	4.27	2.01	0.99985
2.008	0.02193	0.00105	0.095	0.82	0.9909	0.519E-04	4.89	4.14	0.99984
1.854	0.06970	0.00227	0.090	0.81	0.9902	0.510E-04	4.67	9.50	0.99975
1.711	0.13659	0.00374	0.095	0.81	0.9901	0.464E-04	5.06	15.94	0.99970
1.579	0.23900	0.00573	0.100	0.81	0.9900	0.477E-04	5.18	23.19	0.99950
1.458	0.39144	0.00941	0.095	0.81	0.9904	0.662E-04	4.61	30.84	0.99924
1.346	0.57276	0.01404	0.110	0.80	0.9903	0.552E-04	5.76	44.17	0.99904
1.242	0.78299	0.02118	0.115	0.80	0.9903	0.677E-04	6.01	52.07	0.99858
1.147	0.97179	0.03180	0.120	0.79	0.9904	0.825E-04	6.17	62.48	0.99830
1.059	1.11090	0.04055	0.120	0.79	0.9905	0.107E-03	5.77	65.96	0.99785
0.977	1.21547	0.05535	0.125	0.79	0.9902	0.132E-03	5.87	71.52	0.99795
0.902	1.28155	0.10001	0.130	0.77	0.9905	0.215E-03	5.77	80.76	0.99760
0.848									
0.709	1.23797	0.62659	0.150	0.69	0.9901	0.158E-02	4.74	83.44	0.99635
2.479*	0.00140	0.00048	0.070	0.75	0.9908	0.194E-03	2.29	1.08	0.99935
2.275*	0.00307	0.00059	0.075	0.72	0.9908	0.192E-03	2.93	1.05	0.99989
0.832*	1.32901	0.54608	0.115	0.58	0.9900	0.249E-02	3.33	65.80	0.99650

*Scintillator threshold lowered.

Table 4: Electron Arm, 3.384 GeV									
p_0 (GeV)	$(\pi/e)_{raw}$	$(\pi/e)_{in}$	psh/p cut	E/p cut	Tot Cut Eff	$(\pi/e)_f$	γ_{prs}	γ_{cer}	Det Eff
3.028	0.00169	0.00037	0.070	0.85	0.9906	0.946E-04	3.17	1.23	0.99984
2.796	0.00972	0.00055	0.075	0.85	0.9902	0.530E-04	4.45	2.34	0.99982
2.580	0.03115	0.00122	0.075	0.85	0.9906	0.525E-04	4.46	5.22	0.99975
2.382	0.07378	0.00206	0.080	0.84	0.9908	0.372E-04	4.79	11.58	0.99971
2.199	0.15007	0.00336	0.095	0.83	0.9900	0.312E-04	5.62	19.17	0.99961
2.030	0.28172	0.00566	0.095	0.83	0.9903	0.341E-04	5.60	29.67	0.99944
1.873	0.50515	0.00957	0.095	0.83	0.9905	0.450E-04	5.55	38.33	0.99900
1.596	1.20922	0.02446	0.105	0.82	0.9907	0.606E-04	6.09	66.26	0.99824
1.360	2.11551	0.04286	0.115	0.82	0.9905	0.774E-04	6.72	82.38	0.99543
1.159	2.72494	0.07593	0.115	0.81	0.9903	0.133E-03	6.12	93.17	0.99491
0.988	2.90332	0.10919	0.135	0.79	0.9901	0.112E-03	8.23	118.04	0.99350

Table 5: Electron Arm, 4.240 GeV									
p_0 (GeV)	$(\pi/e)_{raw}$	$(\pi/e)_{in}$	psh/p cut	E/p cut	Tot Cut Eff	$(\pi/e)_f$	γ_{prs}	γ_{cer}	Det Eff
3.631	0.00399	0.00040	0.070	0.85	0.9901	0.666E-04	3.82	1.57	0.99986
3.352	0.01839	0.00074	0.070	0.85	0.9904	0.423E-04	4.60	3.81	0.99974
3.086	0.04706	0.00144	0.075	0.84	0.9907	0.367E-04	4.72	8.33	0.99979
2.856	0.09026	0.00219	0.080	0.85	0.9906	0.359E-04	5.21	11.68	0.99979
2.636	0.18018	0.00412	0.075	0.85	0.9907	0.462E-04	4.74	18.80	0.99968
2.433	0.34270	0.00681	0.085	0.83	0.9904	0.416E-04	5.19	31.52	0.99931
2.073	1.02916	0.02079	0.095	0.82	0.9902	0.652E-04	5.69	56.02	0.99845
1.838	1.93423	0.03356	0.095	0.83	0.9906	0.857E-04	5.53	70.78	0.99720
1.767	2.30747	0.04424	0.100	0.82	0.9905	0.101E-03	5.77	75.61	0.99594
1.696	2.73253	0.04630	0.105	0.83	0.9902	0.100E-03	6.17	74.70	0.99563
1.389	4.85001	0.09915	0.100	0.82	0.9904	0.191E-03	5.34	97.16	0.99161

Table 6: Electron Arm, 5.070 GeV									
p_0 (GeV)	$(\pi/e)_{raw}$	$(\pi/e)_{in}$	psh/p cut	E/p cut	Tot Cut Eff	$(\pi/e)_f$	γ_{prs}	γ_{cer}	Det Eff
3.086*	0.20012	0.00488	0.085	0.74	0.9901	0.213E-03	6.11	3.74	0.99981
2.625*	0.67581	0.01574	0.090	0.73	0.9904	0.228E-03	6.46	10.69	0.99946
2.846*	0.38154	0.00814	0.085	0.74	0.9916	0.214E-03	6.11	6.23	0.99965
2.423	1.11029	0.03322	0.065	0.78	0.9902	0.146E-03	4.18	54.44	0.99910
2.233	1.75688	0.05353	0.060	0.78	0.9901	0.245E-03	3.59	60.81	0.99879
2.059	2.65383	0.07926	0.065	0.78	0.9901	0.303E-03	3.71	70.46	0.99794

*scintillator threshold lowered.

5.2 Hadron Arm Results

Here we present only one cut, *Sh/p*, since the Hadron arm does not possess a preshower. As a result the definition of $(\pi/e)_{in}$ changes slightly.

$(\pi/e)_{in}$: π/e after introduction of Shower/p cut.

γ_{sh} : H-Arm Shower cut pion suppression factor.

Table 7: Hadron Arm, 0.862 GeV

p_0 (GeV)	$(\pi/e)_{raw}$	$(\pi/e)_{in}$	Sh/p cut	Shower Cut Ineff	$(\pi/e)_f$	γ_{sh}	γ_{cer}	Det Eff
0.876	0.00141	0.00136	0.240	0.00437	0.129E-02	1.05	1.01	0.99426
0.864	0.00139	0.00133	0.240	0.00465	0.124E-02	1.06	1.01	0.99348
0.851	0.00125	0.00124	0.225	0.00447	0.111E-02	1.11	1.00	0.99283
0.838	0.00148	0.00143	0.240	0.00440	0.133E-02	1.07	1.00	0.99381
0.826	0.00939	0.00954	0.255	0.00488	0.928E-02	1.02	1.01	0.99405
0.808	0.00588	0.00578	0.240	0.00460	0.544E-02	1.05	1.01	0.99202
0.746	0.00775	0.00686	0.165	0.00478	0.532E-02	1.14	1.13	0.99209
0.689	0.01183	0.00936	0.195	0.00492	0.479E-02	1.44	1.36	0.99300
0.587	0.01528	0.00916	0.240	0.00463	0.346E-02	1.69	1.56	0.99330
0.542	0.01622	0.01118	0.255	0.00471	0.444E-02	1.68	1.49	0.99320
0.500	0.01752	0.01306	0.255	0.00473	0.596E-02	1.50	1.46	0.99343
0.461	0.01832	0.01442	0.255	0.00486	0.741E-02	1.38	1.41	0.99342

Table 8: Hadron Arm, 1.720 GeV

p_0 (GeV)	$(\pi/e)_{raw}$	$(\pi/e)_{in}$	Sh/p cut	Shower Cut Ineff	$(\pi/e)_f$	γ_{sh}	γ_{cer}	Det Eff
1.730	0.00097	0.00066	0.210	0.00463	0.429E-03	1.49	1.03	0.99234
1.607	0.00269	0.00200	0.165	0.00445	0.142E-02	1.38	1.02	0.99296
1.484	0.01196	0.00537	0.195	0.00490	0.143E-02	2.32	1.61	0.99154
1.369	0.02147	0.00595	0.210	0.00491	0.665E-03	3.81	2.35	0.99243
1.264	0.04169	0.01098	0.195	0.00449	0.674E-03	4.18	3.90	0.99211
1.167	0.08289	0.01936	0.195	0.00432	0.576E-03	4.86	6.92	0.99224
1.077	0.13333	0.02724	0.210	0.00461	0.491E-03	5.55	9.99	0.99231
0.994	0.17767	0.03756	0.210	0.00445	0.500E-03	5.68	13.23	0.99213
0.918	0.21350	0.05162	0.210	0.00446	0.661E-03	5.38	14.51	0.99222
0.847	0.25632	0.05722	0.225	0.00484	0.562E-03	5.90	17.28	0.99289
0.782	0.29248	0.08544	0.225	0.00485	0.908E-03	4.85	19.40	0.99293

Table 9: Hadron Arm, 2.591 GeV								
p_0 (GeV)	$(\pi/e)_{raw}$	$(\pi/e)_{in}$	Sh/p cut	Shower Cut Ineff	$(\pi/e)_f$	γ_{sh}	γ_{cer}	Det Eff
2.580								
2.530								
2.501	0.00099	0.00068	0.195	0.00420	0.440E-03	1.49	1.03	0.99341
2.357	0.00247	0.00182	0.195	0.00499	0.124E-02	1.38	1.06	0.99260
2.275								
2.175	0.01107	0.00428	0.195	0.00471	0.975E-03	2.71	1.62	0.99110
2.008	0.02544	0.00720	0.195	0.00465	0.745E-03	3.73	2.59	0.99167
1.854	0.07611	0.01649	0.195	0.00445	0.538E-03	4.99	6.14	0.99139
1.711	0.14384	0.02739	0.210	0.00500	0.485E-03	5.68	9.93	0.99174
1.579	0.25466	0.05001	0.195	0.00440	0.495E-03	5.60	18.02	0.99178
1.458	0.41412	0.07226	0.210	0.00493	0.471E-03	6.31	24.29	0.99153
1.346	0.60399	0.10509	0.210	0.00486	0.500E-03	6.35	33.14	0.99174
1.242	0.81953	0.14240	0.210	0.00496	0.572E-03	6.44	38.68	0.99207
1.147	1.02614	0.18254	0.210	0.00471	0.587E-03	6.41	48.53	0.99210
1.059								
0.977	1.31496	0.26489	0.210	0.00459	0.701E-03	6.23	60.67	0.99187
0.902	1.39129	0.33746	0.210	0.00465	0.957E-03	5.65	62.46	0.99199
0.709	1.36351	0.79380	0.210	0.00478	0.641E-02	2.34	52.91	0.99214

Table 10: Hadron Arm, 3.384 GeV								
p_0 (GeV)	$(\pi/e)_{raw}$	$(\pi/e)_{in}$	Sh/p cut	Shower Cut Ineff	$(\pi/e)_f$	γ_{sh}	γ_{cer}	Det Eff
3.028	0.00290	0.00170	0.180	0.00425	0.886E-03	1.73	1.11	0.99209
2.796	0.01275	0.00431	0.180	0.00447	0.847E-03	2.99	1.71	0.99134
2.580	0.03562	0.00930	0.165	0.00448	0.722E-03	3.87	3.33	0.99079
2.382	0.08241	0.01720	0.180	0.00443	0.553E-03	4.85	6.42	0.99146
2.199	0.15930	0.03298	0.165	0.00458	0.553E-03	4.88	12.22	0.99138
2.030	0.29572	0.05486	0.195	0.00468	0.504E-03	5.92	18.37	0.99162
1.873	0.52897	0.09898	0.195	0.00485	0.558E-03	5.91	30.01	0.99107
1.596	1.26122	0.21485	0.210	0.00468	0.650E-03	6.52	50.71	0.99151
1.360	2.21705	0.41592	0.195	0.00439	0.950E-03	6.07	72.19	0.99098
1.159	2.91210	0.59041	0.195	0.00433	0.114E-02	5.90	87.49	0.99159
0.988	3.12122	0.82965	0.195	0.00479	0.184E-02	5.14	87.68	0.99135

Table 11: Hadron Arm, 4.240 GeV								
p_0 (GeV)	$(\pi/e)_{raw}$	$(\pi/e)_{in}$	Sh/p cut	Shower Cut Ineff	$(\pi/e)_f$	γ_{sh}	γ_{cer}	Det Eff
3.086	0.05039	0.01226	0.150	0.00473	0.624E-03	4.15	4.74	0.99123
2.856	0.09577	0.02267	0.150	0.00498	0.656E-03	4.26	8.10	0.99135
2.636	0.18969	0.04624	0.135	0.00428	0.721E-03	4.14	15.49	0.99165
2.636	0.18694	0.04159	0.150	0.00493	0.662E-03	4.54	13.83	0.99136
2.433	0.35814	0.08532	0.135	0.00418	0.764E-03	4.24	26.33	0.99139
2.073	1.05488	0.22663	0.150	0.00497	0.966E-03	4.73	49.59	0.99072
1.838	2.02404	0.50041	0.135	0.00458	0.173E-02	4.13	69.98	0.99100
1.767	2.42085	0.59964	0.135	0.00445	0.188E-02	4.13	77.18	0.99066
1.696	2.84828	0.71682	0.135	0.00439	0.219E-02	4.08	80.04	0.99164
1.389	5.09934	2.23827	0.120	0.00429	0.923E-02	2.34	103.45	0.99070

Table 12: Hadron Arm, 5.070 GeV								
p_0 (GeV)	$(\pi/e)_{raw}$	$(\pi/e)_{in}$	Sh/p cut	Shower Cut Ineff	$(\pi/e)_f$	γ_{sh}	γ_{cer}	Det Eff
3.086	0.20330	0.04455	0.150	0.00489	0.652E-03	4.61	14.81	0.99056
2.846	0.38430	0.08340	0.150	0.00487	0.755E-03	4.67	23.67	0.99060
2.625	0.68544	0.15962	0.135	0.00435	0.948E-03	4.35	38.69	0.99139
2.423	1.10970	0.26107	0.135	0.00436	0.114E-02	4.32	53.24	0.99068
2.233	1.79044	0.42460	0.135	0.00430	0.150E-02	4.31	65.85	0.99099
2.059	2.68318	0.72439	0.120	0.00429	0.239E-02	3.79	79.79	0.99022

References

[1] A. Keitikyan et al., *About Shower Detector Software*, JLAB hypertext document. http://www.cebaf.gov/~armen/sh_web_page/sh_page_init.html

[2] *Review of Particle Physics*,Table 25.4, July 1998

[3] K. Slifer,*Analysis of the Hall A HRS Čerenkov Detectors for E94010*, E94010 Technical note .

[4] H. Fender et al., *The Hall A Operating Manual* , JLAB hypertext document. http://hallaweb.jlab.org/document/OPMAN-old/node152.html